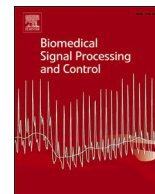Contents lists available at ScienceDirect

Biomedical Signal Processing and Control

journal homepage: www.elsevier.com/locate/bspc

Diagnosis of cardiotocographic sinusoidal patterns by spectral analyses

Ricardo Savirón-Cornudella [a,b], Antonio Laliena Bielsa [c], Javier Esteban-Escaño [d], Javier Calvo Torres [a], Marta Chóliz Ezquerro [e], Berta Castán Larraz [f], Elisa Díaz de Terán Martínez-Berganza [g], María José Rodríguez Castaño [h], Miguel Álvaro Navidad [i], Mercedes Andeyro García [j], Jaime Whyte Orozco [k], Sergio Castán Mateo [f], Luis Mariano Esteban [c,l,1,*]

[a] Department of Obstetrics and Gynecology, Hospital Clínico San Carlos, Spain
[b] Instituto de Investigación Sanitaria San Carlos (IdISSC), Universidad Complutense, Calle del Prof Martín Lagos, S/N, 28040 Madrid, Spain
[c] Departament of Applied Mathematics, Escuela Universitaria Politécnica de La Almunia, Universidad de Zaragoza, 50100 La Almunia de Doña Godina, Spain
[d] Department of Electronic Engineering and Communications, Escuela Universitaria Politécnica de La Almunia, Universidad de Zaragoza, Zaragoza, 50100 La Almunia de Doña Godina, Spain
[e] Department of Obstetrics, Dexeus University Hospital, Barcelona, Spain
[f] Department of Obstetrics and Gynecology, Miguel Servet University Hospital, Isabel La Católica 3, 50009 Zaragoza, Spain
[g] Department of Obstetrics and Gynecology, Zarzuela University Hospital, Madrid, Spain
[h] Department of Neonatology, Hospital Clínico San Carlos, Universidad Complutense, Calle del Prof Martín Lagos, 28040 Madrid, S/N, Spain
[i] Department of Obstetrics and Gynecology, Hospital Fundación Jimenez Diaz, Madrid, Spain
[j] Department of Obstetrics and Gynecology, Villalba University General Hospital, Madrid, Spain
[k] Departamento de Anatomía e Histología Humanas, Universidad de Medicina de Zaragoza, Zaragoza, Spain
[l] Institute for Biocomputation and Physics of Complex Systems (BIFI), Universidad de Zaragoza, 50009 Zaragoza, Spain

ARTICLE INFO

ABSTRACT

Background: The sinusoidal pattern in cardiotocographic (CTG) monitoring shows a sinus-shaped signal longer than 30 min without short-term variability. It is commonly linked to fetal morbidity, particularly severe fetal anemia. Pseudosinusoidal patterns resemble sinusoidal patterns but without adverse fetal outcomes. This study aims to characterise sinusoidal and pseudosinusoidal patterns using spectral analysis.
Methods: A multicenter study case-control was conducted between January 2012 and February 2023. Maternal characteristics, perinatal data, and CTG parameters through spectral analysis were examined. The spectrum of the electrocardiographic signal was calculated, and the proportion of energy (PE), short- and long-term variability, amplitude, and the differences between sinusoidal, pseudosinusoidal, and control groups were compared. A predictive model for signal type was built using a classification tree.
Results: 60 CTG records were collected, including 38 controls. Of the 13 sinusoidal patterns detected, all exhibited a sinusoidal pattern with a PE ratio > 0.3, 9 of them (69 %) had a PE ratio > 0.5, and 4 (31 %) were in the range of 0.3–0.5. Among the 9 cases diagnosed as pseudosinusoidal, all had a sinusoidal pattern with a PE within the range of 0.3–0.5. Every control exhibited a PE < 0.3, except for one case. Short-term variability demonstrated limited discriminatory capability, while long-term variability showed a strong discriminatory capacity. For the classification tree, accuracy diagnosis was 92.3 %, 88.8 %, and 97.3 % for the sinusoidal, pseudosinusoidal, and control groups, respectively.
Conclusion: Computerised spectral analysis and the variable PE within the frequency range of 1.8–3.5 are reliable parameters to discriminate sinusoidal patterns.

1. Introduction

Cardiotocographic (CTG) monitoring is currently the universal method for the surveillance of intrapartum fetal well-being. It involves continuous monitoring of both the fetal heart rate (FHR) and maternal uterine contraction (UC) signals, which are acquired, processed, and displayed using complex electronic devices [1].

During the intrapartum period, an ultrasound transducer is typically used for external FHR monitoring. The transducer contains piezoelectric effect crystals that convert electrical energy into ultrasound waves, which are then directed towards the fetal heart. The ultrasound waves bounce off the cardiac structures and return to the transducer, where they are converted back into electrical signals. The Doppler effect is used to detect the movements of the cardiac structures and determine the FHR [2,3].

Central monitoring systems have been developed to allow simultaneous display of multiple tracings on several locations, making it easier to monitor the fetal signals. The rate and pattern of the FHR are displayed on a computer screen for later analysis. This monitoring method has proven to be effective in detecting fetal distress and guiding obstetric interventions to improve fetal outcomes, given that certain FHR signal patterns are associated with adverse perinatal outcomes [4].

The typical or true sinusoidal pattern, initially described by Manseau in association with severe fetal anemia [5], is generally defined as a pattern with a sinusoidal-shaped signal equidistant from the baseline. It is characterised by a stable basal fetal heart rate between 120 and 160 beats per minute (bpm), an amplitude from 5 to 15 bpm, a frequency from 2 to 5 cycles per minute, reduced or absent short-term variability [6–8] lasting more than 30 min with no accelerations [9], and may occasionally present late decelerations [7,10].

Although the pathophysiology is still not fully understood, it seems that this sinusoidal shape is attributed to the lack of central nervous system control over the heart [10] and is mainly secondary to severe fetal anemia or hypovolemia, acute or chronic. Moreover, sinusoidal shape has also been observed in cases of preeclampsia, diabetes, infections, or other fetal malformations [11]. Traditionally, the most common cause of "true sinusoidal patterns" has been hemolytic anemia due to Rh isoimmunization [12], although its incidence has significantly decreased due to Anti-D immunoglobulin [10]. Currently, it is found more frequently in cases of fetomaternal transfusions (FMTs), feto-fetal transfusion syndromes in monochorionic twin pregnancies, bleeding due to fetal scalp blood sampling, cordocentesis, placental abruption, or rupture of vasa previa [11–13].

Patterns lacking all the characteristics of true sinusoidals, as some authors argue, can be classified as "atypical sinusoidal patterns" with less smooth "saw teeth" morphology [7] or "shark teeth" morphology [12,14]. On the other hand, "pseudosinusoidal patterns" are similar to sinusoidal patterns, although they are limited in time and do not mean adverse fetal effects [12] While they may lead to confusion regarding their differentiation from sinusoidal patterns, "saw teeth" have also been described in them [9].

The definition and classification of sinusoidal patterns have been the subject of intense debate [6,7,12]. Furthermore, the definition of "pseudosinusoidal patterns" has not been clearly established, prompting some authors to suggest the reclassification of previous publications [8]. Given these considerations, including the presence of inter- and intra-observer variability [15–22], there is a need for more objective diagnostic and differentiation methods. Computational approaches have been suggested, including studies involving spectral analysis [23] and fractal dimension analysis [24] for sinusoidal patterns diagnosis.

Therefore, given that the sinusoidal pattern has demonstrated a clear association with severe fetal issues, its identification from the signal is a crucial objective. Equally important is the differentiation from pseudosinusoidal patterns, which have a lesser impact on fetal well-being. Our objective was to investigate an extensive series of cases with sinusoidal-like pattern, along with their perinatal outcomes, and employ time and spectral measures to define their characteristics. We aimed to formulate a predictive model capable of classifying FHR signals as either sinusoidal, pseudosinusoidal, or normal based on the frequency spectrum.

2. Related work

Central monitoring systems enable healthcare providers to observe fetal signals, these systems display real-time continuous recordings of the FHR and uterine contractions. The recorded signals are available for further analysis and documentation [4].

Da Silva Neto et al. deliver a comprehensive review within this context, exploring a broad spectrum of methodologies offered by machine learning algorithms for the analysis of FHR data [25]. In this prediction context, it can be distinguished between studies that provide a complete computer-aided diagnosis system, [26–28], and those which use the signal to improve the fetal state detection [29–42].

Comert et al. [26] presents a prototype of open-access software designed for the analysis of cardiotocography, referred to as CTG-OAS. This software encompasses key functionalities, including database access, preprocessing, feature transformation, and automated CTG analysis classification. Moreover, the investigation delves into the effectiveness of texture features such as contrast, correlation, energy, and homogeneity for the detection of fetal hypoxia. Anisha et al. [27] constructs a system for the detection of Fetal Cardiac Anomalies that emphasizes the extraction of fetal electrocardiogram (FECG) signals and the identification of pathological fetuses. This system relies on clinically crucial features concealed within the amplitudes and waveform durations of the FECG signals. Zhao et al. [28] introduced a computer-aided diagnosis (CAD) system incorporating an advanced deep learning (DL) algorithm. The 1-dimensional preprocessed FHR signal was transformed into a 2-dimensional image using recurrence plot (RP) to capture non-linear characteristics effectively. The enriched image dataset, obtained by varying RP parameters, was subsequently utilized to train a convolutional neural network (CNN).

Concerning models utilizing the FHR signal for predicting adverse perinatal outcomes, a diverse array of algorithms has been employed. These algorithms included decision trees [34], random forest [22], support vector machines [30–32,34], artificial neural networks [30,34,28–31], K-nearest neighbor [30], convolutional neural networks [33,35,36,38,42], fuzzy approach [32,41], Naïve Bayes [32], deep Gaussian processes [37], and deep-ANFIS models [41]. The consideration of these algorithms aims to enhance the accuracy of predicting fetal acidemia, whether based on the FHR signal itself or the features extracted from it. Overall, machine learning algorithms present promising avenues for improvement in this predictive domain.

Additionally, deep learning models have been proposed to analyze time series in other fields. Xiao et al. [43] introduced a dual-stage Multivariate Time Series (MTS) methodology intended to improve the effectiveness of convolution operations. This approach incorporates a convolution layer for extracting spatial correlation within the MTS, and a Long Short-Term Memory (LSTM) model is employed to capture temporal correlation. The integration of an attention mechanism with LSTM proves effective in addressing the challenge of insufficient temporal dependency in MTS prediction. Also, Xiao et al. [44] developed an adaptive fused spatial–temporal graph structure, encapsulating concealed temporal, spatial, and spatial–temporal dependencies among individual instances within the MTS. The model employs the AFSTGC module to effectively process the disordered correlation features inherent in the MTS.

3. Material and methods

3.1. Sample selection

A retrospective case-control multicenter study was conducted at several hospitals in Spain, including Miguel Servet University Hospital

in Zaragoza, Villalba General University Hospital, San Carlos Clinical Hospital, and La Zarzuela University Hospital in Madrid, between January 2012 and February 2023. Experts from each of the participating hospitals identified and recruited records with a sinusoidal-like appearance, categorising them into sinusoidal and pseudosinusoidal patterns. We defined a typical sinusoidal-like pattern based on the literature [6–10]. Such patterns are characterized by a stable baseline fetal heart rate between 120 and 160 beats per minute (bpm), an amplitude of 5 to 15 bpm (or sometimes higher), a frequency of 2 to 5 cycles per minute, and reduced or absent short-term variability with no accelerations. Conversely, an atypical sinusoidal pattern lacks some of the typical characteristics. A pattern that resembles a sinusoidal pattern but is self-limited [12] or does not exhibit the characteristics of a fluctuating sine wave around and equidistant from the baseline is categorized as pseudosinusoidal.

Control samples (normal patterns) were collected, excluding those with maternal and perinatal adverse outcomes (such as fetal anemia, fetal acidemia with cord arterial pH < 7.05, FIRS, preeclampsia, or diabetes). The investigation received approval from the Clinical Research Ethics Committee of Fundación Jiménez Díaz, Hospital La Zarzuela, and Hospital Clínico San Carlos de Madrid (CEIm-FJD, PI EO131-20).

Maternal characteristics, including maternal age, parity, maternal pathology, and maternal risk factors, were collected. Additionally, perinatal data, such as gestational age, neonatal weight and weight percentile [45], fetus sex, 5-minute Apgar scores, umbilical artery blood gases, neonatal severe anemia (defined as hematocrit < 30 %) [46], and cases of fetal inflammatory response syndrome (FIRS), were recorded. The recording periods for the sinusoidal and pseudosinusoidal cases were collected, with a minimum duration of 15 min. In the case of pseudosinusoidal records, the data were collected prior to returning to normality. As for the control group, data from the 30 min before delivery were also considered.

3.2. Spectral study

Fetal heart rate (FHR) records are typically contaminated with artifacts and temporal gaps due to maternal, fetal, or transducer movements. We employed an artifact elimination algorithm similar to the one introduced by Bernardes et al. in 1991 [47]. In the case of large temporal gaps, we trimmed the signal, while for smaller gaps, we applied linear interpolation. Subsequently, to enable the application of frequency domain techniques, we resampled the signal using linear interpolation to achieve a frequency of fs = 10 Hz (i.e., 10 samples per second).

We calculated the trend curve T_x for each signal x by employing a central moving mean over one minute (equivalent to 600 samples). Furthermore, we computed the energy spectrum, which is the squared modulus of the Discrete Fourier Transform (DFT), calculated through the Fast Fourier Transform (FFT), for the detrended signal, $x_d = x - T_x$.

Using the spectrum of the signal, we defined the following features to characterise sinusoidal and pseudosinusoidal patterns.

3.2.1. Proportion of energy (PE)

To identify the dominant frequency range [fa,fb] we measured the energy concentration between the frequencies fa and fb and we used the proportion of accumulated energy in that range:

$$PE_{f_a,f_b} = 2 \frac{\sum_{f_a \leq f_k \leq f_b} |\widehat{x_d}(f_k)|^2}{\sum_{f_k} |\widehat{x_d}(f_k)|^2}$$

where $\widehat{x_d}(f_k)$ is the value at frequency f_k of the DFT of the detrended signal x_d. The factor of 2 in the above expression is a consequence of the symmetry of the energy spectrum. The values of $PE_{2.5}$ are expected to be higher in records with sinusoidal and pseudosinusoidal patterns.

3.2.2. Reduced or absent short-term variability

We evaluated short-term variability (variability associated with frequencies above f_b) using a measure similar to that used to study the dominant frequency: $PE_{f_b,f_s/2}$. Note that $f_s/2$ is the maximum observable frequency due to resampling. We expected to find that in records with a sinusoidal pattern, the short-term variability is lower compared to a normal (normal case) record and a record with a pseudosinusoidal pattern.

3.2.3. Long-term variability

We measured long-term variability using the ℓ^2 norm

$$\|x\|_2 = \sqrt{\sum_{i=0}^{N-1} |x_i|^2}$$

for a signal $x = \{x_i\}_{i=0}^{N-1}$. Note that $\|x\|_2$ represents the energy of the signal (according to the Plancherel theorem [48], energy in the time domain and frequency domain coincide except for a scaling factor N). Specifically, we use the energy of the centered trend curve, averaged over its duration

(since not all signals have equal duration):

$$VT = \sqrt{\frac{\|T_x - \overline{T_x}\|_2^2}{N}}$$

where T_x is the trend curve of signal x (calculated using a central moving mean over one minute) and N is the length of T_x. By using the square root, VT is measured in beats per minute (BpM). VT quadratically measures the area enclosed between the trend curve and its mean. Records with sinusoidal and pseudosinusoidal patterns expected to exhibit lower long-term variability. Low long-term variability is an indirect measure of baseline stability.

3.2.4. Amplitude

We estimated the amplitude of a sinusoidal pattern as half the range between the 5th and 95th percentiles of the detrended signal. By not using the full range of the signal (which would provide the amplitude in the case of an ideal sinusoidal pattern), we eliminated possible outliers.

3.3. Statistical analysis

A descriptive analysis of signal spectrum features was conducted based on the patterns classified by the experts: sinusoidal, pseudosinusoidal, and normal. Since none of the features exhibited a normal distribution, we summarised the variables using the median and interquartile range. To compare characteristics among groups, we used the Kruskal-Wallis test. Additionally, we employed scatterplots to illustrate differences among categories based on the four variables derived from the signal and their respective spectra.

Furthermore, we constructed a predictive model for signal type using a classification tree. Classification trees are recursive partition models that aim to minimise the impurity of the classes defined by the partition [49]. They provide a straightforward classification system that is easy to implement. In this study, we used the Gini index as the loss function and set the minimum number of observations required for a split to 10 within a node. Additionally, we specified the minimum number of observations in any terminal node as 3 and limited the maximum depth of any node in the final tree to 30. The model is visualized in a tree diagram and a scatterplot. We evaluated the model's accuracy using a confusion matrix and subsequently calculated sensitivity and specificity by dichotomizing signals using the sinusoidal, pseudosinusoidal, and normal groups in different analyses.

To assess the impact of predictor variables on signal prediction, we developed the Variable Importance (VIMP) plot. The VIMP quantifies the difference in prediction error when a predictor is perturbed by applying a permutation that assigns the variable to a terminal node

different from its original assignment, following the Breiman–Cutler Variable VIMP approach [50].

4. Results

In the study, experts identified 22 cases classified as having a sinusoidal-like pattern: 13 were categorised as sinusoidal and 9 as pseudosinusoidal. For these cases and the 38 controls (normal cases), the electrocardiographic signal was processed, and its spectrum was calculated, as depicted in Fig. 1. The energy spectrum exhibits a clear accumulation of energy in the form of a peak or plateau between frequencies fa = 1.8 and fb = 3.5 cycles per minute for records with sinusoidal and pseudosinusoidal patterns. Thus, the Potential Energy was calculated within the frequency interval [1.8, 3.5]. The results are presented in Table 1, and additional figures can be found in Fig. 1 Supplementary.

Of the 13 cases diagnosed as sinusoidal by experts, all exhibited a positive sinusoidal pattern with a PE ratio greater than 0.3. Specifically, 9 (69 %) had a PE ratio exceeding 0.5, and 4 cases (31 %) had a PE ratio falling within the range of 0.3–0.5. Out of these cases, 11 (85 %) were associated with neonatal anemia, one case (7.5 %) was diagnosed with FIRS, and one case was associated with preeclampsia (7.5 %). Among the 11 cases with neonatal anemia, 7 were identified as having a positive Kleihauer test, indicative of fetomaternal transfusion (FMT). One case was diagnosed with anemia due to isoimmunization in a twin pregnancy, and the cause of the remaining three anemia cases could not be determined, as the Kleihauer test was not performed in two of these cases. In terms of perinatal outcomes, 8 out of 12 cases (67 %) had acidosis with an arterial blood umbilical cord pH below 7.10, were small for gestational age with a birth weight percentile below 10, and/or had an Apgar score below 7 at five minutes. There was one neonatal death in a case of severe anemia at birth with an atypical intrapartum sinusoidal pattern.

Of the 9 cases diagnosed by experts as pseudosinusoidal, all displayed a positive sinusoidal pattern with PE falling within the range of 0.3–0.5 and exhibited self-limiting behavior. Four (45 %) of these cases were associated with the use of the analgesic drug pethidine for pain management during labor. In terms of perinatal outcomes, none of the cases had a pH below 7.10, were small for gestational age or preterm, and none required postnatal transfusion or experienced complications necessitating prolonged hospitalization.

Regarding the control cases, all of them displayed a spectrum with PE values under 0.3, except for one case that had a PE range of 0.3–0.5, which was considered a false positive for the sinusoidal pattern. Thus, PE in the range of 1.8–3.5 shows a high discriminatory ability between groups (Fig. 2 Supplementary). Short-term variability exhibited limited discriminatory capability when distinguishing between normal and pseudosinusoidal patterns, spanning a broad range of 0.05–0.4. Sinusoidal patterns, on the other hand, primarily fell within a narrower interval (0.05–0.15), except for one distinct case (Case 13) (Fig. 3 Supplementary). Long-term variability demonstrated a strong discriminatory capacity between sinusoidal-pseudosinusoidal and normal cases, with minimal overlap occurring within the interval of (5,10), except in Case 13. However, this variable was unable to effectively discriminate between sinusoidal and pseudosinusoidal cases (Fig. 4 Supplementary). The amplitude showed a similar performance (Fig. 5 Supplementary).

4.1. Classification tree

The description of signal features by groups is presented in Table 2, revealing significant differences between them in all spectrum features. All the features were considered predictor variables in constructing a classification tree, which is depicted in Fig. 2.

The most critical variable to classify signals was the PE in the frequency interval [1.8, 3.5]. A PE less than 0.2965 classified the signals as normal; a PE falling within the range of (0.2965, 0.4792); and short-term variability greater than 0.0992 classified the signals as pseudosinusoidal. Signals were classified as sinusoidal if they met either of the following criteria: a PE greater than or equal to 0.4792 or a PE within the range of (0.2965, 0.4792) and short-term variability less than or equal to 0.0992. A scatterplot in Fig. 3 visually represents the recursive partition. The Variable Importance (VIMP) plot in Fig. 4 ranks the importance of variables in the classification tree.

The accuracy in classification is presented in the confusion matrix in Table 3, with a detection rate of 92.3 %, 88.8 %, and 97.3 % for the sinusoidal, pseudosinusoidal, and normal groups, respectively. The sensitivity to classify records as sinusoidal or pseudosinusoidal cases was 100 %, and the specificity was 97.3 %. Therefore, the predictions accurately classify individuals into the three study classes and also successfully dichotomize cases as either normal or sinusoidal-pseudosinusoidal.

5. Discussion

We have illustrated that specific signal characteristics, encompassing both temporal and frequency domains, contribute to the identification of authentic sinusoidal and pseudosinusoidal heart rate patterns.

Using exploratory analysis, the highest number of cycles observed for sinusoidal spectral patterns was 3.5 cycles per minute, slightly below the reported up to 5 cycles per minute in prior studies. Manseu et al. [5] reported 11 cases with the oscillation frequency of 2–4 cycles per minute, Kubli et al. [6] noted SHR pattern with oscillation frequency of 2–5 cycles per minutes in 12 patients and Graça et al. [7] reported 8 cases in the frequency interval (2,5). Additionally, we obtained amplitudes below 8.1 BpM, significantly less than the values mentioned in the FIGO Consensus [9]. Moreover, the computerized evaluation of PE was the most important variable to distinguish between sinusoidal patterns linked to adverse perinatal effects and pseudosinusoidal patterns lacking such effects.

5.1. Sinusoidal patterns

Currently, sinusoidal patterns remain underdiagnosed due to their low incidence (0.3–1.7 %) [13] and the diagnostic challenges they pose, often intercalated with atypical patterns, which were the most common cases in our study [8]. It's important to note that a perfect sinusoid is only clearly visible when the CTG paper speed is set at 3 cm/min [9]. However, in our cases (as in most European centers), the paper speed is 1 cm/min, resulting in a more compact sinusoid.

The primary cause of sinusoidal patterns is fetal anemia, currently attributed to fetomaternal transfusion (FMT) [10]. It has also been described in association with chorioamnionitis, diabetes, and preeclampsia [11,51]. Our results align with previous publications, with the majority of our cases being associated with fetal anemia due to FMT, one case of FIRS, and one case of preeclampsia. Additionally, sinusoidal patterns more frequently showed an association with low Apgar scores at 5 min, low arterial pH in the umbilical cord, small for gestational age, prematurity, and an elevated baseline frequency compared to pseudosinusoidal patterns.

In our study, all sinusoidal cases were identified as sinusoidal patterns with PE in the frequency interval (1.8, 3.5) > 0.4792, with the exception of four cases. One of these cases probably involved a combination of a chronic hypoxia pattern [10] secondary to anemia (case 4), another exhibited an atypical sinusoidal pattern with numerous decelerations (case 9), and cases 12 and 13 were associated with FIRS and preeclampsia, respectively. Differentiating between typical and atypical sinusoidal patterns is challenging due to the low number of typical patterns and the signal noise.

5.2. Pseudosinusoidal patterns

The definition of pseudosinusoidal patterns has been a subject of controversy, as previous works have referred to what other authors
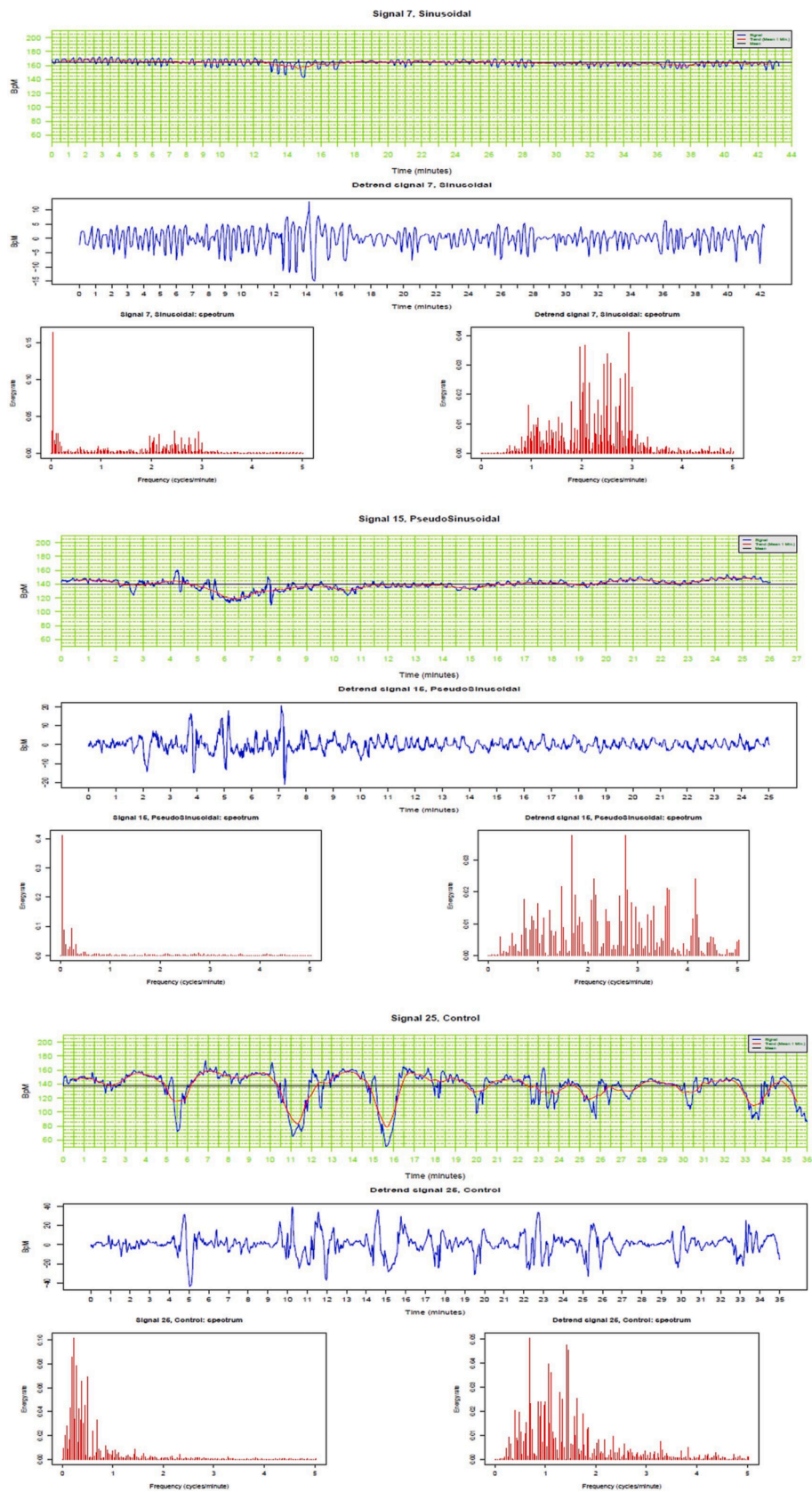
Fig. 1. Examples of signal modeling and spectrogram generation.

Table 1
Perinatal outcomes associated with sinusoidal patterns and cases of pseudosinusoidal patterns.

Case	Weeks of delivery	Neonatal weight	pH arterial	Apgar 5 min	Hematocrit (%)	Kleihauer test	Cause suspicion	Type	PE (1.8,3.5)	PE > 3.5	LT variability	Amplitude
1	39 2/7	2880 (21)	7.28	8	13	Positive	FMT	Sinusoidal atypical	0.69	0.05	1.96	1.41
2	36 4/7	1959 (0)	7.19	9	11.8	Positive	FMT	Sinusoidal atypical	0.59	0.08	3.10	2.40
3	40 6/7	3560 (59)	7.09	6	9.7	Positive	FMT	Sinusoidal atypical	0.50	0.06	5.87	8.06
4	40	3200 (37)	7.26	6	<10	Np	Unknown (neonatal death)	Sinusoidal atypical	0.40	0.03	8.20	11.24
5	37	2115 (1)	7.05	8	11.5	Positive	FMT	Sinusoidal atypical	0.68	0.06	0.69	1.00
6	38 2/7	3160 (62)	7.18	5	13.9	Np	Unknown	Sinusoidal atypical	0.58	0.12	1.95	2.66
7	31 1/7	1600 (32)	7.26	7	23.4	Positive	FMT	Sinusoidal typical	0.65	0.09	2.19	4.74
8	40 1/7	3130 (19)	7.09	7	10.5	Positive	FMT	Sinusoidal atypical	0.57	0.09	4.38	5.30
9	40 2/7	2830 (10)	7.21	6	15	Positive	FMT	Sinusoidal atypical	0.37	0.09	5.31	1.61
10	38 2/7	3060 (42)	7.30	9	<15	Negative	FMT	Sinusoidal atypical	0.51	0.14	3.73	3.08
11	35	2260, 1780 (47, 3)	7.36; 7.22	8; 3	28; 20	Negative	Isoimmunization (coombs positive)	Sinusoidal atypical	0.63	0.06	2.50	4.01
12	37 3/7	3000 (61)	7.25	3	44	Negative	FIRS	Sinusoidal atypical	0.48	0.08	2.00	3.50
13	37 4/7	2810 (38)	7,16	10	56	Np	Preeclampsia	Sinusoidal atypical	0.30	0.38	18.40	9.74
14	40 4/7	3310 (48)	7.42	10	Np	Np		Pseudosinusoidal	0.37	0.17	2.71	3.49
15	41 1/7	4250 (96)	7.15	5	Np	Np	Pethidine	Pseudosinusoidal	0.36	0.35	6.22	4.77
16	39 3/7	2860 (18)	7.18	10	Np	Np		Pseudosinusoidal	0.48	0.07	3.70	7.33
17	41 4/7	3770 (81)	7.21	10	Np	Np		Pseudosinusoidal	0.38	0.11	4.72	6.37
18	40 6/7	4250 (97)	7.20	10	Np	Np	Pethidine	Pseudosinusoidal	0.31	0.22	3.96	4.26
19	41 3/7	3490 (58)	7.33	9	Np	Np	Pethidine	Pseudosinusoidal	0.33	0.29	4.67	7.58
20	39	3470 (99)	7.25	9	Np	Np	Pethidine	Pseudosinusoidal	0.44	0.34	2.01	7.11
21	39	3030 (35)	7.26	10	44	Np		Pseudosinusoidal	0.37	0.25	3.70	5.14
22	39 4/7	3420 (65)	7.21	10	Np	Np		Pseudosinusoidal	0.46	0.36	1.14	2.62
23	37 5/7	2425 (6)	7.14	10	Np	Np		Normal	0.11	0.09	12.57	23.42
24	41 5/7	3010 (10)	7.29	10	Np	Np		Normal	0.10	0.09	16.05	27.22
25	41 4/7	2820 (4)	7.33	10	Np	Np		Normal	0.17	0.10	15.65	17.99
26	41 3/7	3270 (28)	7.26	10	Np	Np		Normal	0.18	0.26	6.59	7.23
27	41	2725 (4)	7.15	7	Np	Np		Normal	0.08	0.15	19.40	18.41
28	41	3560 (60)		10	Np	Np		Normal	0.28	0.36	15.00	17.35
29	39 6/7	3020 (23)	7.3	10	Np	Np		Normal	0.23	0.27	5.12	2.74
30	40 6/7	3550 (61)	7.3	10	Np	Np		Normal	0.21	0.36	11.30	14.90
31	36 2/7	2280 (11)	7.22	10	Np	Np		Normal	0.14	0.09	12.28	16.34
32	41 6/7	3580 (50)	7.34	10	Np	Np		Normal	0.16	0.28	13.77	10.40
33	40	3300 (51)	7.24	10	Np	Np		Normal	0.17	0.29	28.13	16.75
34	40 6/7	3360 (42)	7.31	10	Np	Np		Normal	0.21	0.20	16.18	18.55
35	41	3860 (84)	7.25	10	Np	Np		Normal	0.19	0.24	8.67	8.56
36	40 2/7	2690 (4)	7.16	10	Np	Np		Normal	0.11	0.19	20.51	15.67
37	41 2/7	4060 (92)	7.26	10	Np	Np		Normal	0.24	0.38	13.79	12.75
38	39 4/7	3555 (76)	7.07	7	Np	Np		Normal	0.11	0.13	17.07	10.76
39	41 5/7	3790 (73)	7.26	10	Np	Np		Normal	0.25	0.38	13.74	18.11
40	41 3/7	3160 (20)	7.2	8	Np	Np		Normal	0.21	0.23	18.16	10.79
41	41 5/7	3370 34)	7.36	9	Np	Np		Normal	0.24	0.14	8.77	10.62
42	39 2/7	3280 (57)	7.08	9	Np	Np		Normal	0.18	0.10	15.84	14.23
43	40 3/7	3160 (29)	7.16	10	Np	Np		Normal	0.23	0.21	9.33	11.80
44	39 2/7	2440 (2)	7.18	9	Np	Np		Normal	0.10	0.07	21.12	22.94
45	40 3/7	2620 (3)	7.2	70	Np	Np		Normal	0.09	0.17	18.44	14.74
46	40 1/7	3855 (90)	7.21	8	Np	Np		Normal	0.29	0.20	16.00	7.08
47	40 6/7	3060 (18)	7.24	9	Np	Np		Normal	0.23	0.25	14.35	14.83
48	41 1/7	3690 (70)	7.32	9	Np	Np		Normal	0.25	0.21	10.89	9.72
49	40	3595 (75)	7.08	10	Np	Np		Normal	0.32	0.22	7.31	15.53
50	38 2/7	3330 (78)	7.34	9	Np	Np		Normal	0.06	0.13	12.86	15.42
51	39	3940 (98)	7.22	10	Np	Np		Normal	0.10	0.08	10.55	15.07
52	38	3700 (97)	7.27	10	Np	Np		Normal	0.11	0.06	11.93	11.19
53	41 1/7	2980 (11)	7.26	10	Np	Np		Normal	0.26	0.31	12.40	14.29
54	41 5/7	4400 (98)	7.09	10	Np	Np		Normal	0.21	0.31	5.48	7.95
55	40 1/7	3400 (56)	7.21	10	Np	Np		Normal	0.23	0.18	14.56	29.36
56	39	2800 (16)	7.17	3	Np	Np		Normal	0.28	0.31	25.51	16.45
57	40 1/7	2950 (16)	7.13	10	Np	Np		Normal	0.13	0.18	30.26	13.87
58	41 4/7	4090 (91)	7.08	10	Np	Np		Normal	0.16	0.12	15.64	19.69
59	38 3/7	2320 (4)	7.25	10	Np	Np		Normal	0.11	0.20	21.70	17.92
60	35	2680 (81)	7.20	9	Np	Np		Normal	0.10	0.11	14.33	7.03

Bpm: beats per minutes, Np: Not performed, FIRS: fetal inflammatory response syndrome, FMT: feto-maternal transfusion.

considered atypical sinusoidals as pseudosinusoidals [8,11,13]. Typically, pseudosinusoidal patterns last less than 30 min [11], but in some cases, they can extend up to 60 min [52]. In our study, all cases were resolved in less than 1 h, and none of the sinusoidal cases were self-limited. Pseudosinusoidal patterns are self-limiting or transient, although they may recur during monitoring. These patterns maintain variability and may resemble "saw teeth," similar to sinusoidal "saw teeth," which can sometimes make their distinction difficult [7,9,11] These patterns may be secondary to maternal opioid analgesia, as seen in several of our cases, epidural analgesia [13,53], or more commonly, fetal sucking or other mouth movements, as demonstrated postnatally [9,12].

All cases diagnosed as pseudosinusoidal patterns were detected as sinusoidal patterns by spectral analysis, but none of them had PE in the frequency interval (1.8, 3.5) above 0.3. As our study has shown, this variable has the highest ability to detect sinusoidal and pseudosinusoidal patterns. There was only one case that was identified as pseudosinusoidal by spectral analysis, and it was a control case. Therefore, this case was considered a false positive in the spectral study.

5.3. Computerized analyses and multinomial classification

Logistic regression has been frequently employed to integrate FHR parameters. Marti et al. [54] demonstrated that the combination of

Table 2
Descriptive analysis of spectrum features by type of signal categories.

Variable	Sinusoidal n = 13	Pseudosinusoidal n = 9	Normal n = 38	p-value
Proportion of energy in (1.8,3.5) frequencies	0.57 (0.48,0.63)	0.37 (0.36,0.44)	0.18 (0.11,0.23)	<0.001
Proportion of energy for frequencies above 3.5	0.08 (0.06,0.09)	0.37 (0.36,0.44)	0.20 (0.12,0.27)	<0.001
Long-term variability	3.10 (2.00,5.30)	3.70 (2.71,4.67)	14.34 (11.45,16.84)	<0.001
Amplitude	3.50 (2.40,5.30)	5.14 (4.26,7.11)	14.86 (10.76,17.78)	<0.001

deceleration area with maternal–fetal characteristics yielded a notable discrimination ability of 0.83 in predicting acidemia. Similarly, Cahill et al. [55] obtained comparable results, achieving an Area Under the Curve (AUC) of 0.77 by combining total deceleration area, instances of tachycardia, and episodes of moderate variability. In a study by Choliz-Ezquerro et al. [56], the analysis of total reperfusion time or inter-deceleration time resulted in a model with an AUC of 0.826.

CTG monitoring should be regarded as a dynamic process rather than a static classification based on morphological features [57]. With the digitalization of the FHR signal, it becomes feasible to process it using CNNs or more intricate encoder–decoder deep learning architectures for acidemia prediction.

In the study by Tang et al. [42], the MKNet model is introduced, utilizing a CNN to achieve an impressive AUC value of 0.95. The author suggests its potential application in real-time fetal health monitoring using portable devices. Similarly, Zhao et al. [33] employs a CNN approach and attains an AUC above 0.95 through a 10-fold cross-validation procedure for predictive purposes. Although computer-aided diagnosis systems exhibit lower predictive abilities, Cömert et al. [26] reports a sensitivity of 76.83 % and specificity of 78.27 %, whereas Anisha et al. [27] demonstrates an AUC of 0.96 for detecting cardiac anomalies. Esteban et al. [58] compares machine learning models, identifying a random forest with a sensitivity of 90 % and specificity of 89 % as the best-performing model. In a similar vein, Zhao et al. [33] employs an AdaBoost model, achieving a sensitivity of 92 % and specificity of 90 %. On the contrary, Iraji et al. [41] attains near-perfect classification results using neural networks, with a sensitivity of 99 % and specificity of 97 %. Nonetheless, these exceptionally high values would benefit from external validation for further confirmation.

Regarding sinusoidal pattern prediction, in the year 2000, Suzuki et al. conducted a study involving a power spectral analysis of R-R interval variability in four fetal lambs at 120 to 130 days' gestation [59]. To induce a sinusoidal heart rate pattern, the researchers administered atropine sulfate and arginine vasopressin. The purpose of the study was to examine potential changes in the very low-frequency area (0.01–0.025 cycles/beat), which corresponds to the frequency of the sinusoidal heart rate pattern. The results of the study indicated that there were no significant changes in the very low-frequency area, suggesting that the sinusoidal heart rate pattern remained unchanged despite the administration of atropine sulfate and arginine vasopressin.
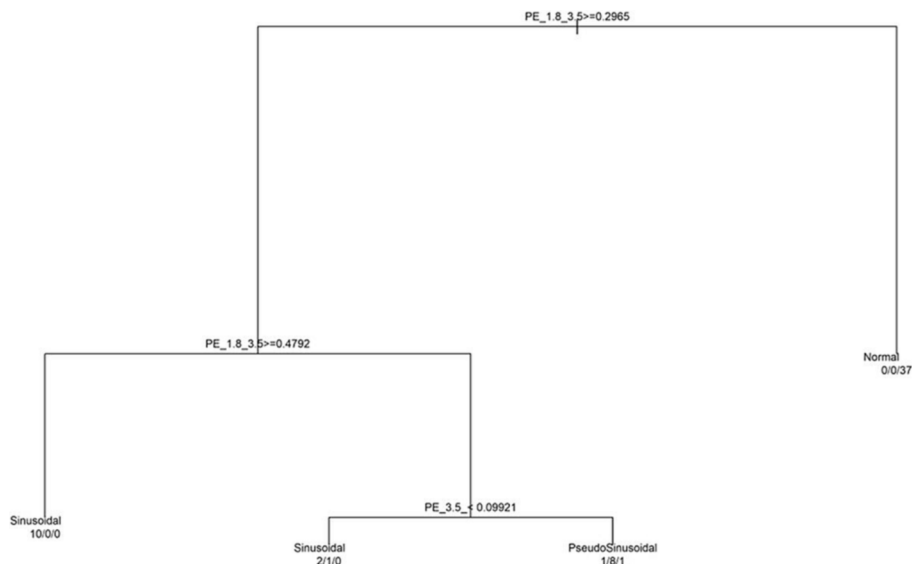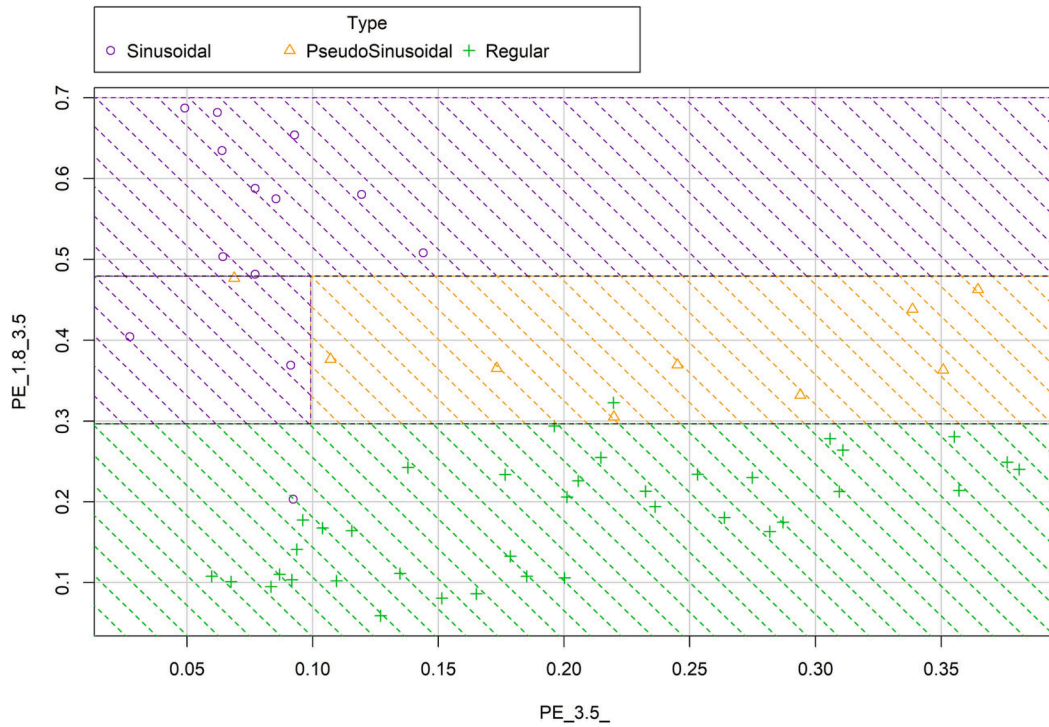

Fig. 2. Classification tree.

Fig. 3. Scatterplot of the 60 cases distributed by Proportion of energy in the interval frequency (1.8,3.5) and Proportion of energy_3.5_.
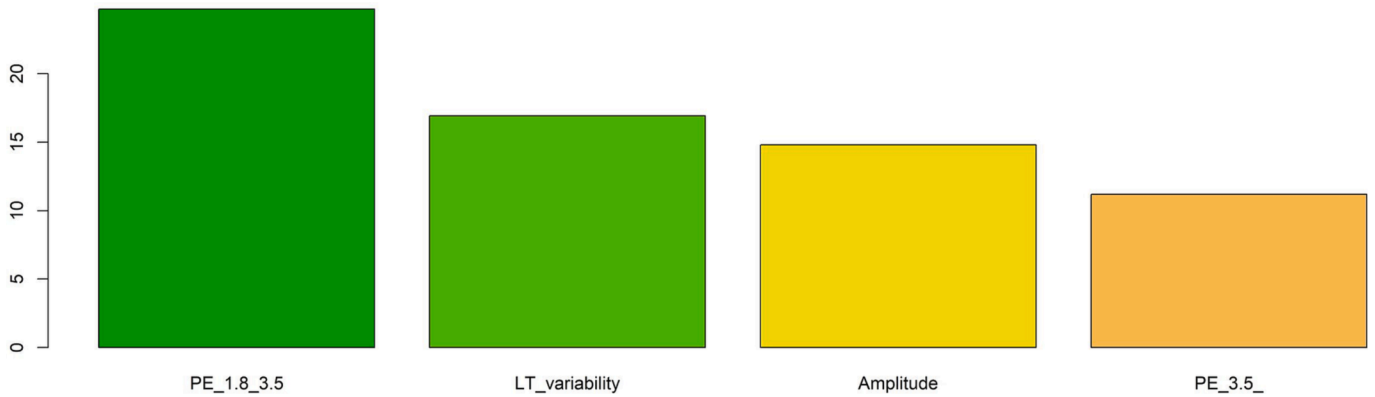

Fig. 4. Variable importance plot of the classification tree.

Table 3
Confusion matrix of the classes predicted by the classification tree.

		Predicted classes		
		Sinusoidal	Pseudosinusoidal	Normal
Real classes	Sinusoidal	12	1	0
	Pseudosinusoidal	1	8	0
	Normal	0	1	37

In 2005, Maeda et al. conducted a study [23] using spectral methods to analyse nine cases of fetal sinusoidal heart rate (FSHR) with adverse effects (fetal-neonatal anemia, death, or severe asphyxia), seven cases of sinusoidal FSHR without adverse effects, and five cases of normal fetal heart rate (FHR). The study focused on several variables, including peak power spectrum frequency (PPSF), peak power spectrum density (PPSD), the area under the power spectrum of 0.03125–0.1 Hz (La), the area under the entire power spectrum (Ta), and the ratio of La/Ta (%). The researchers found that cases of fetal sinusoidal heart rate associated with adverse perinatal effects were clearly distinguishable from physiologic FSHR and normal FHR based on the La/Ta ratio and PPSD. The La/Ta ratio and PPSD were significantly larger in the pathologic fetal sinusoidal heart rate. While Maeda used only spectral measures and distinguished only two groups, FSHR cases with adverse outcomes and FSHR cases plus controls without adverse outcomes.

In the course of our investigation, we employed measurements within both the frequency and time domains with the objective of discerning and categorizing signals into three distinct types: sinusoidal, pseudosinusoidal, and normal [23]. This categorization holds particular significance for our study, as uncertainties may arise in instances where the visual differentiation between sinusoidal and pseudosinusoidal signals proves to be challenging, particularly in the context of management considerations.

In the year 2019, Wu et al. [24] conducted a study focusing on sinusoidal fetal heart rate patterns detected by expert obstetricians. In this study, the researchers developed a segmentation model for fetal sinusoidal heart rate based on a combination of the standard deviation of the period and the fractal dimension. The model exhibited excellent

performance on the test set, achieving a classification accuracy of more than 97 %. However, it is important to note that this particular study did not differentiate between sinusoidal patterns associated with perinatal effects and those that were not associated with them.

Multiple studies of the sinusoidal pattern of fetal heart rate have been performed. In a systematic review by Castro et al. in 2021 [60], it was concluded that the spectral analysis of the fetal heart rate is a simple and powerful tool that may become an adjunctive method to CTG, helping healthcare professionals to accurately identify fetuses at risk of intrapartum hypoxia and to implement timely obstetrical interventions to reduce the incidence of related adverse perinatal outcomes.

Several studies have also shown promising results for using machine learning or computerised algorithms to analyse fetal heart rate patterns. Future research directions could involve investigating the potential benefits of using computer algorithms to improve the accuracy of diagnosing fetal heart rate patterns [22,55,61].

Visual diagnosis of these patterns is a complex process, often subjective, especially in cases such as sinusoidal patterns that are infrequent (although with high neonatal morbidity and mortality), requiring a significant amount of expertise and experience to detect them. In situations where the detection of a sinusoidal spectral pattern is challenging or when differentiating between a true sinusoidal pattern and a pseudosinusoidal pattern is uncertain, especially in cases lasting over 30 min, computerized spectral analysis offers a valuable tool to provide conclusive information and, if necessary, facilitate further spectral testing. Our prediction was based on a classification tree that used simple features derived from the signal spectral analysis, with significant differences between the groups in all spectrum features. These differences confirm that all the features are valuable predictors to classify signals as sinusoidal, pseudosinusoidal, or normal. This can be easily implemented as a diagnostic tool, providing alerts for suspected pseudosinusoidal and sinusoidal patterns. Prospective studies are required to corroborate the data and assess the implementation of a more objective test to detect these patterns in electronic heart rate monitoring in real time to improve perinatal adverse effects.

5.4. Strengths and limitations

Although the incidence of fetal anemia is low, our study has analysed one of the highest series of sinusoidal cases to date. Furthermore, we have proposed a simple classification method to differentiate between sinusoidal and pseudosinusoidal patterns using spectral analysis, with the predictor variable being the PE in the frequency interval (1.8, 3.5). This frequency range had not been utilized previously, as the usual range mentioned in the literature is typically from 2 to 5 cycles per minute [6].

The main innovation of this study lies in the multiclass prediction approach, where the decision tree has proven to be an effective tool owing to its model simplicity and adaptive capabilities. This feature not only facilitates ease of implementation but also enhances its suitability for integration into routine clinical practice.

6. Conclusion

In conclusion, through the use of spectral analysis, the variable "proportion of energy" within the frequency range 1.8–3.5 seems to be a valuable marker to distinguish sinusoidal patterns with adverse perinatal effects. Additionally, we have proposed a simple and highly accurate classification system for the detection of sinusoidal, pseudosinusoidal, and normal cases. These parameters, which differentiate each type of signal, can be easily implemented within birthing centers, offering valuable contributions to the diagnosis and management of cases where a sinusoidal pattern is suspected. In situations where the detection of a sinusoidal pattern is challenging or when differentiation between a true sinusoidal pattern and a pseudosinusoidal pattern is uncertain, especially in cases lasting over 30 min. Computerised spectral analysis provides a valuable tool to offer conclusive

information in sinusoidal patterns.

CRediT authorship contribution statement

Ricardo Savirón-Cornudella: Writing – review & editing, Writing – original draft, Conceptualization. **Antonio Laliena Bielsa:** Writing – review & editing, Writing – original draft, Methodology, Data curation. **Javier Esteban-Escaño:** Writing – review & editing, Investigation. **Javier Calvo Torres:** Writing – review & editing, Investigation. **Marta Chóliz Ezquerro:** Writing – review & editing, Investigation. **Berta Castán Larraz:** Writing – review & editing, Investigation. **Elisa Díaz de Terán Martínez-Berganza:** Writing – review & editing, Investigation. **María José Rodríguez Castaño:** Writing – review & editing, Investigation. **Miguel Álvaro Navidad:** Writing – review & editing, Investigation. **Mercedes Andeyro García:** Writing – review & editing, Investigation. **Jaime Whyte Orozco:** Writing – review & editing, Investigation. **Sergio Castán Mateo:** Writing – review & editing, Visualization, Investigation, Conceptualization. **Luis Mariano Esteban:** Writing – review & editing, Writing – original draft, Methodology, Data curation.

Declaration of competing interest

The authors declare that they have no known competing financial interests or personal relationships that could have appeared to influence the work reported in this paper.

Data availability

Data will be made available on request.

Acknowledgements

Appendix A. Supplementary data

Supplementary data to this article can be found online at https://doi.org/10.1016/j.bspc.2024.106174.

References

[1] I. Nunes, D. Ayres-de-Campos, Computer analysis of foetal monitoring signals, Best Pract. Res. Clin. Obstet. Gynaecol. 30 (2016) 68–78.

[2] D. Ayres-de-Campos, Z. Nogueira-Reis, Technical characteristics of current cardiotocographic monitors, Best Pract. Res. Clin. Obstet. Gynaecol. 30 (2016) 22–32.

[3] M. Docker, Doppler ultrasound monitoring technology, BJOG Int. J. Obstet. Gynecol 100 (1993) 18–20.

[4] I. Nunes, D. Ayres-de-Campos, C. Figueiredo, J. Bernardes, An overview of central fetal monitoring systems in labour, J. Perinat. Med 41 (2013) 93–99.

[5] P. Manseau, J. Vaquier, J. Chavinié, C. Sureau, Le rythme cardiaque foetal "sinusoïdal". aspect évocateur de souffrance foetale au cours de la grossesse, J Gynecol Obstet Biol Reprod (paris) 1 (1972) 343–352.

[6] H.D. Modanlou, R.K. Freeman, Sinusoidal fetal heart rate pattern: its definition and clinical significance, Am J Obstet Gynecol 142 (1982) 1033–1038.

[7] L.M. Graça, C.G. Cardoso, C. Calhaz-Jorge, An approach to interpretation and classification of sinusoidal fetal heart rate patterns, Eur J Obstet Gynecol Reprod Biol 27 (1988) 203–212.

[8] D.E. Neesham, M.P. Umstad, R.B. Cincotta, D.L. Johnston, G.M. McGrath, Pseudosinusoidal fetal heart rate pattern and fetal anaemia: case report and review, Aust N Z J Obstet Gynaecol 3 (1993) 386–388.

[9] D. Ayres-de-Campos, C.Y. Spong, E. Chandraharan, FIGO intrapartum fetal monitoring expert consensus panel FIGO consensus guidelines on intrapartum fetal monitoring: cardiotocography, Int J Gynaecol Obstet 13 (2015) 13–24.

[10] S. Pereira, E. Chandraharan, Recognition of chronic hypoxia and pre-existing foetal injury on the cardiotocograph (CTG): urgent need to think beyond the guidelines, Porto Biomed J 2 (2017) 124–129.

[11] H.D. Modanlou, Y. Murata, Sinusoidal heart rate pattern: reappraisal of its definition and clinical significance, J Obstet Gynaecol Res 30 (2004) 169–180.

[12] N. Yanamandra, E. Chandraharan, Saltatory and sinusoidal fetal heart rate (FHR) patterns and significance of FHR "overshoots", CWHR 9 (2014) 175–182.

[13] K.W. Murphy, V. Russell, A. Collins, P. Johnson, The prevalence, aetiology and clinical significance of pseudo-sinusoidal fetal heart rate patterns in labour, Br J Obstet Gynaecol 98 (1991) 1093–1101.

[14] A. Pinas, E. Chandraharan, Continuous cardiotocography during labour: analysis, classification and management, Best Pract Res Clin Obstet Gynaecol 30 (2016) 33–47.

[15] C. Hernandez Engelhart, K. Gundro Brurberg, K.J. Aanstad, A.S.D. Pay, A. Kaasen, E. Blix, S. Vanbelle, Reliability and agreement in intrapartum fetal heart rate monitoring interpretation: a systematic review, Acta Obstet Gynecol Scand. 102 (8) (2023) 970.

[16] C. Zamora, M. Chóliz, I. Mejía, E. Díaz de Terán Martínez-Berganza, L.M. Esteban, A. Rivero Alonso, B. Castán, M. Andeyro, R. Saviron Cornudella, Diagnostic capacity and interobserver variability in FIGO, ACOG, NICE and chandraharan cardiotocographic guidelines to predict neonatal acidemia, J. Matern. Fetal Neonatal Med. 80 (2021) 6479.

[17] P.V. Nielsen, B. Stigsby, C. Nickelsen, J. Nim, Intra- and inter-observer variability in the assessment of intrapartum cardiotocograms, Acta Obstet Gynecol Scand 66 (1987) 421–424.

[18] M.D. Beaulieu, J. Fabia, B. Leduc, B.J. Brisson, A. Bastide, D. Blouin, R.J. Gauthier, A. Lalonde, The reproducibility of intrapartum cardiotocogram assessments, Can Med Assoc J 127 (1982) 214–216.

[19] E. Blix, O. Sviggum, K.S. Koss, P. Oian, Inter-observer variation in assessment of 845 labour admission tests: comparison between midwives and obstetricians in the clinical setting and two experts, BJOG 110 (2003) 1–5.

[20] H.A. Zain, J.W. Wright, G.E. Parrish, S.J. Diehl, Interpreting the fetal heart rate tracing. Effect of Knowledge of Neonatal Outcome, J Reprod Med 43 (1998) 367–370.

[21] L. Hruban, J. Spilka, V. Chudáček, P. Janků, M. Huptych, M. Burša, A. Hudec, M. Kacerovský, M. Koucký, M. Procházka, V. Korečko, J. Seget'a, O. Šimetka, A. Měchurová, L. Lhotská, Agreement on intrapartum cardiotocogram recordings between expert obstetricians, J. Eval. Clin. Pract. 21 (4) (2015) 694–702.

[22] A. Ugwumadu, S. Arulkumaran, A second look at intrapartum fetal surveillance and future directions, J Perinat Med. 51 (2022) 135–144.

[23] K. Maeda, T. Nagasawa, Automatic computerized diagnosis of fetal sinusoidal heart rate, Fetal Diagn Ther. 20 (5) (2005) 328–334.

[24] W. Wu, Y. Zhang, Y. Lv, W. Yu and Y. Lin, Shape Pattern Based Sinusoidal Fetal Heart Rate Detection from Scanned CTG Records, 2019 IEEE 15th International Conference on Control and Automation (ICCA), Edinburgh, UK, (2019) 1320-1325.

[25] M.G. Da Silva Neto, J.P. Do Vale Madeiro, D.G. Gomes, On designing a biosignal-based fetal state assessment system: a systematic mapping study, Comput. Methods Programs Biomed. 216 (2022) 106671.

[26] Z. Cömert, A.F. Kocamaz, Open-access software for analysis of fetal heart rate signals, Biomed. Signal Process. Control 45 (2018) 98–108.

[27] M. Anisha, S.S. Kumar, E.E. Nithila, M. Benisha, Detection of fetal cardiac anomaly from composite abdominal electrocardiogram, Biomed. Signal Process. Control 65 (2021) 102308.

[28] Z. Zhao, Y. Zhang, Z. Comert, Y. Deng, Computer-aided diagnosis system of fetal hypoxia incorporating recurrence plot with convolutional neural network, Front. Physiol. 10 (2019) 255.

[29] W. Alsaggaf, Z. Cömert, M. Nour, K. Polat, H. Brdesee, M. Toğaçar, Predicting fetal hypoxia using common spatial pattern and machine learning from cardiotocography signals, Appl. Acoust. 167 (2020) 107429.

[30] O. Barquero-Pérez, R. Santiago-Mozos, J.M. Lillo-Castellano, B. García-Viruete, R. Goya-Esteban, A.J. Caamaño, J.R. Rojo-Alvarez, C. Martín-Caballero, Fetal heart rate analysis for automatic detection of perinatal hypoxia using normalized compression distance and machine learning, Front. Physiol. 8 (2017) 113.

[31] Z. Cömert, A.F. Kocamaz, V. Subha, Prognostic model based on image-based time-frequency features and genetic algorithm for fetal hypoxia assessment, Comput. Biol. Med. 99 (2018) 85–97.

[32] S. Das, S.M. Obaidullah, K.C. Santosh, K. Roy, C.K. Saha, Cardiotocograph-based labor stage classification from uterine contraction pressure during ante-partum and intra-partum period: a fuzzy theoretic approach, Health Information Science and Systems 8 (2020) 1–13.

[33] Z. Zhao, Y. Deng, Y. Zhang, Y. Zhang, A. Zhang, L. Shao, DeepFHR: intelligent prediction of fetal acidemia using fetal heart rate signals based on convolutional neural network, BMC Med. Inf. Decis. Making 19 (2019) 1–15.

[34] Z. Cömert, A. Şengür, Ü. Budak, A.F. Kocamaz, Prediction of intrapartum fetal hypoxia considering feature selection algorithms and machine learning models, Health Information Science and Systems 7 (2019) 1–9.

[35] A. Petrozziello, C.W.G. Redman, A.T. Papageorghiou, I. Jordanov, A. Georgieva, Multimodal convolutional neural networks to detect fetal compromise during labor and delivery, IEEE Access 7 (2019) 112026–112036.

[36] Z. Cömert, A.F. Kocamaz, Fetal hypoxia detection based on deep convolutional neural network with transfer learning approach, in: R. Silhavy (Ed.), Software

[37] Engineering and Algorithms in Intelligent Systems, CSOC2018 Computer Science on-Line Conference, Springer International Publishing, Cham, 2019, pp. 239–248.

[37] G. Feng, J.G. Quirk, P.M. Djurić, Supervised and unsupervised learning of fetal heart rate tracings with deep gaussian processes, in: 2018 14th Symposium on Neural Networks and Applications (NEUREL). (2018) 1–6.

[38] P. Fergus, C. Chalmers, C.C. Montanez, D. Reilly, P. Lisboa, B. Pineles, Modelling segmented cardiotocography time-series signals using one-dimensional convolutional neural networks for the early detection of abnormal birth outcomes, IEEE Transactions on Emerging Topics in Computational Intelligence (2020) 1–11.

[39] W. Gao, Y. Lu, Fetal heart baseline extraction and classification based on deep learning, in: 2019 International Conference on Information Technology and Computer Application (ITCA) (2019) 211–216.

[40] M.A. Ma'sum, P. Riskyana Dewi Intan, W. Jatmiko, A.A. Krisnadhi, N.A. Setiawan, I.M.A.D. Suarjaya, Improving deep learning classifier for fetus hypoxia detection in cardiotocography signal, in: 2019 International Workshop on Big Data and Information Security (IWBIS) (2019) 51–56.

[41] M.S. Iraji, Prediction of fetal state from the cardiotocogram recordings using neural network models, Artif. Intell. Med. 96 (2019) 33–44.

[42] H. Tang, T. Wang, M. Li, X. Yang, The design and implementation of cardiotocography signals classification algorithm based on neural network, Comput. Math. Methods Med. 2018 (2018) 8568617.

[43] Y. Xiao, H. Yin, Y. Zhang, H. Qi, Y. Zhang, Z. Liu, A dual-stage attention-based conv-LSTM network for spatio-temporal correlation and multivariate time series prediction, Int. J. Intell. Syst. 36 (5) (2021) 2036–2057.

[44] Y. Xiao, K. Xia, H. Yin, Y.D. Zhang, Z. Qian, Z. Liu, L. Yuehan, X. Li, AFSTGCN: prediction for multivariate time series using an adaptive fused spatial-temporal graph convolutional network, Digital Communications and Networks (2022).

[45] R. Savirón-Cornudella, L.M. Esteban, D. Lerma, L. Cotaina, A. Borque, G. Sanz, S. Castan, Comparison of fetal weight distribution improved by paternal height by spanish standard versus intergrowth 21st standard, J Perinat Med 46 (2018) 750–759.

[46] R.D. Christensen, D.K. Lambert, V.L. Baer, D.S. Richards, S.T. Bennett, S.J. Ilstrup, E. Henry, Severe neonatal anemia from fetomaternal hemorrhage: report from a multihospital health-care system, J Perinatol 33 (2013) 429–434.

[47] J. Bernardes, C. Moura, J.P. de Sa, L.P. Leite, The Porto system for automated cardiotocographic signal analysis, J Perinat Med. 19 (1–2) (1991) 61–65.

[48] M. Plancherel, M. Leffler, Contribution À L'Étude de la reprÉsentation D'une fonction arbitraire par des integrales definies, Rend. Circ. Matem. Palermo 30 (1910) 289–335.

[49] L. Breiman, J. Friedman, C.J. Stone, R.A. Olshen, Classification and Regression Trees, Routledge, 1984.

[50] H. Ishwaran, M. Lu, Standard errors and confidence intervals for variable importance in random forest regression, classification, and survival, Stat. Med. 38 (2019) 558–582.

[51] N. Gleicher, C.D. Runowicz, B.L. Brown, Sinusoidal fetal heart rate pattern in association with amnionitis, Obstet Gynecol 56 (1980) 109–112.

[52] J.H. Gray, D.W. Cudmore, E.R. Luther, T.R. Martin, A.J. Gardner, Sinusoidal fetal heart rate pattern associated with alphaprodine administration, Obstet Gynecol 52 (1978) 678–681.

[53] G.J. Hofmeyr, E.W. Sonnendecker, Sinusoidal versus pseudosinusoidal fetal heart rate patterns, S Afr Med J 64 (1983) 19–23.

[54] S. Martí, M. Lapresta, J. Pascual, C. Lapresta, S. Castán, Deceleration area and fetal acidemia, J. Matern. Fetal Neonatal Med 30 (2017) 2578–2584.

[55] A.G. Cahill, M.G. Tuuli, M.J. Stout, J.D. López, G.A. Macones, A prospective cohort study of fetal heart rate monitoring: deceleration area is predictive of fetal acidemia, Am. J. Obstet. Gynecol 218 (523) (2018) e1–523.e12.

[56] M. Chóliz, R. Savirón, L.M. Esteban, C. Zamora, A. Espiau, B. Castán, S. Castán Mateo, Total intrapartum fetal reperfusión time (fetal resilience) and neonatal acidemia, J. Matern. Fetal Neonatal Med 91 (2021) 5977.

[57] C. Garabedian, J. De Jonckheere, L. Butruille, P. Deruelle, L. Storme, V. Houfflin-Debarge, Understanding fetal physiology and second line monitoring during labor, J. Gynecol. Obstet. Hum. Reprod. 46 (2017) 113–117.

[58] L.M. Esteban, B. Castán, J. Esteban-Escaño, G. Sanz-Enguita, A.R. Laliena, A.C. Lou-Mercadé, M. Choliz, S. Castán, R. Savirón-Cornudella, Machine learning algorithms combining slope deceleration and fetal heart rate features to predict acidemia, Appl. Sci. 13 (13) (2023) 7478.

[59] T. Suzuki, K. Okamura, Y. Kimura, T. Watanabe, N. Yaegashi, J. Murotsuki, S. Uehara, A. Yajima, Power spectral analysis of R-R interval variability before and during the sinusoidal heart rate pattern in fetal lambs, Am J Obstet Gynecol. 182 (5) (2000) 1227–1232.

[60] L. Castro, L.M. Loureiro, T.S. Henriques, I. Nunes, Systematic review of intrapartum fetal heart rate spectral analysis and an application in the detection of fetal acidemia, Front Pediatr. 9 (2021) 661400.

[61] A. Georgieva, P. Abry, I. Nunes, M.G. Frasch, Editorial: fetal-maternal monitoring in the age of artificial intelligence and computer-aided decision support: a multidisciplinary perspective, Front Pediatr. 10 (2022) 100779.